Optimization, preparation and characterization of rutin-quercetin dual drug loaded keratin nanoparticles for biological applications

Selvaraj Kunjiappan [1]; Anindita Chowdhury [2]; Balasubramanian Somasundaram [1]; Chiranjib Bhattacharjee [2]; Selvam Periyasamy [1]*

[1]*Sir CV Raman- KS Krishnan International Research Centre, Kalasalingam University, Krishnankoil, India*
[2]*Department of Chemical Engineering, Jadavpur University, Kolkata, India*

ABSTRACT

Objective(s): Response surface methodology (RSM) by central composite design (CCD) was applied to statistically optimize the preparation of Rutin-Quercetin (Ru-Qr) dual drug loaded human hair keratin nanoparticles as well as evaluate the characteristics.

Materials and Methods: The effects of three independent parameters, namely, temperature (X_1:10-40 C), surfactant (X_2: SDS (1), SLS (2), Tween-20 (3)), and organic solvents (X_3: acetone (1), methanol (2), chloroform (3)) were investigated to optimize the preparation of dual drug loaded keratin nanoparticles, and to understand the effects of dependent parameters namely, drug releasing capacity, average particle size, total antioxidant power, zeta potential, and polydispersity index of Ru-Qr nanoparticles. Optimization was executed by CCD and RSM using statistical software (Design Expert, version 8.0.7.1, Stat-Ease, Inc., Minneapolis, MN, USA). The optimal Ru-Qr dual drug loaded keratin nanoparticles were obtained at temperature (X_1): 40ÚC, SDS (X_2), and acetone (X_3).

Results: Under this conditions to achieve highest drug releasing capacity of 98.3%, average size of nanoparticles are 125 nm, total antioxidant power 98.68%, zeta potential 28.09 mV, and polydispersity index of 0.54. Although majority of the experimental values were relatively well matched with the predicted values.

Conclusion: This optimization study could be useful in pharmaceutical industry, especially for the preparation of new nano-therapeutic formulations encapsulated with drug molecules. This nanotechnology based drug delivery system is to overcome multi drug resistance and site specific action without affecting other organs and tissues. The methodology adopted in this work shall be useful in improvement of quality of human health.

Keywords: *Keratin, Quercetin, Response surface methodology, Rutin*

INTRODUCTION

Recently the exploration in drug delivery via nanoparticulate system has given rise to technological innovation in the field of biomedicine [1]. The development of nanomedicine has given a crucial impulse for the fabrication of various nanovehicles such as liposomes, nanoparticles, nanocapsules, etc., for the treatment of degenerative disorders [2]. Among the several nanovectors employed for drug delivery system, nanoparticles have gained interest in comparison to microspheres due to its high surface to volume ratio, small size and ease of penetrating into cells [3]. Nanoparticles are engineered from organic as well as inorganic source. Inorganic nanoparticles such as gold, silver, titanium, iron are widely explored for the fabrication of diagnostic and therapeutic tool [4]. On the other hand organic materials include natural biopoly-

✉ *Corresponding Author Email: selvaraj.k@klu.ac.in*
Tel: (+91) *9994972108*

mers with many key advantages such as high payload, biodegradability, immunocompatibility and controlled release profile can be represented as one of the promising tool for treatment of many diseases [5].

Among the biopolymers protein nanoparticle has been recognized as suitable candidate for targeted delivery of drug. The ease of surface modification of protein and the presence of functional groups on its surface enables tumor targeting at specific site [6]. Proteins inherently carry positive or negative charges at pH above or below the isoelectric point. This favors the drug loading with different charges. The hydrophobic domains of protein also attract hydrophobic drug which represents protein as a potential carrier of drug [7]. Moreover, they are taken up efficiently by the cells by interacting with protein receptors in tumor cells and are accumulated at the tumor site [8]. Proteins such as albumin, gliadin, zein, whey protein, and gelatin have been investigated by researchers. These proteins suffer from poor stability in aqueous environment which restrict its therapeutic application. To enhance the stability and hydrophilicity of the protein, surface modification by coupling with cross linkers or targeting ligands can be one of the feasible strategies. Whereas, avoiding the complications involved with cross linking and employing a protein which is intrinsically stable in aqueous environment could be an alternate strategy [9].

Keratin is one such water-stable, biocompatible protein polypeptide found in hair, nails, horns of animals, feathers of birds [10]. It has a structural resemblance with collagen. The tripeptides in keratin Arg-Gly-Asp and Leu-Asp-Val enables high affinity for binding the cell surface receptor and ligands. The presence of cysteine and highly cross linked structural organisation may be a cause for its water stability [11, 12]. As a potent candidate of biomaterials it has been used as a capping agent of silver nanoparticles, scaffold for bone tissue regeneration, haemostatic agent and protective agent in biomedical applications [13]. Therefore, it can serve as an effective carrier agent for the drug delivery system.

Apart from the carrier, drug loading is another important aspect that needs to be considered for the fabrication of a drug delivery system. The development of drug resistance over a course of therapy leads to the administration of multiple drugs which in turn worsens the condition and causes inconvenience to the patients along with reducing

the efficacy of the drug. The advent of dual drug delivery system has evolved as a promising approach in the field of regenerative medicine [14]. The simultaneous delivery of two different drugs in a controlled manner through a single system is more convenient for the patients. In this current scenario researchers have explored the synergistic effect of co-delivery of curcumin and platinum in polymeric micelle [15], calcium phosphate (CP) nanocarriers dual-loaded with bovine serum albumin (BSA) and hydrophobic drug ibuprofen (IBU) [16]. So far keratin has not been used as a carrier for drug loading and drug delivery systems. This feature article discusses the use of keratin for the co-delivery of flavonoids rutin and quercetin complexes.

The objective of this present study was to optimize, prepare and characterize dual drug (Ru-Qr) loaded nanoparticles, and to stabilize the particles from harsh conditions and different pH in the gastrointestinal tract, they were microencapsulated by water-stable carrier, keratin. Encapsulation of flavonoids into keratin was a major challenge as the hydrophilic flavonoid has a tendency to separate into the aqueous phase during synthesis. So, there is a pressing need to study effects of several process variables for obtaining maximum entrapment efficiency and minimum particle sizes nanoparticles. A conventional approach for optimization of multivariate is done by using one variable at a time. Response surface methodology can solve simultaneously multivariate equations, proved to a useful software tool for solving multivariable system. Therefore, the experiment was designed by response surface methodology using central composite design. All the obtained data were analyzed by using statistical software (Design Expert, version 8.0.7.1, stat-ease, Inc., Minneapolis, MN, USA). We also hypothesize that, optimization studies could yield the large scale production of nanoparticles with desired features paving way for pharmaceutical preparations and ease their massive applications.

EXPERIMENTAL
Materials

Human hair was collected from beauty salon, Sundarapandiam, nearby Kalasalingam University, Krishanankoil, India. Rutin, quercetin, 2-mercaptoethanol, Tris-Hcl, thiourea, sodium lauryl sulphate, Bradford protein assay reagent, tween-20,

SDS were procured from Himedia Laboratories Pvt. Ltd. Mumbai, India. 2, 2-diphenyl-1-picrylhydrazyl (DPPH), sephadex, phosphate buffered saline (PBS) were obtained from Sigma–Aldrich, MO, USA; and analytical grade solvents of Merck, Mumbai, India were used in the study.

The glass wares (BOROSIL) supplied by Ganapathy scientific suppliers, Srivilliputtur, India, were used. These were washed with dilute nitric acid and thoroughly rinsed with double distilled water and dried in hot air oven with before use.

Extraction of Keratin

Extraction of keratin from human hair was carried out according to the method described by Akira Nakamura et al. [17] with slight modifications. Discarded human hair was washed extensively with detergent, and air-drying at room temperature. The dried hair was washed with ethanol, and external lipids were removed using a mixture of chloroform/methanol (2 : 1, v/v) for 24 h.

The delipidized hair (20 g) was mixed with a solution (50 mL) containing 25 mM Tris–HCl, pH 8.5, 2.6 M thiourea, 5 M urea and 5% 2-mercaptoethanol (2-ME) at 50 °C for 1-3 days. The mixture was filtered and centrifuged at 15000 X g for 20 minutes at room temperature. The obtained supernatant was used as a hair protein fraction.

Estimation of protein

The amount of protein extracted from human hair was determined by the colorimetric method of Bradford method using the Himedia protein assay reagent.

Preparation of Ru-Qr nanoparticles by solid dispersion method

A Ru-Qr dual drug loaded nanoparticles was prepared by solid dispersion method. Briefly, 1 mg of Rutin and 1 mg of Quercetin was dissolved in 10 mL of organic solvent (acetone or methanol or chloroform) under sonication. Further this organic phase was added in a drop wise manner to 50 mL of ultra-pure water containing 1mg of keratin and with 5 mg of surfactant (SDS or Sodium lauryl sulphate or Tween-20) under magnetic stirrer. Nanoparticles thus formed turned the solution turbid. Organic solvent was removed by continuous overnight stirring. Resultant nanoparticles were separated by ultracentrifugation. Obtained nanoparticles were washed three times with ultrapure water and used for further characterization.

Characterization of Nanoparticles
Measurement of antioxidant power

The total antioxidant power of dual drug loaded keratin nanoparticles was measured by 2, 2-diphenyl-1-picrylhydrazil (DPPH) free radical scavenging assay method with some modifications [18]. Prepared Ru-Qr loaded keratin nanoparticles colloidal solution (0.1 mL) was added to 3 mL of ethanolic solution of DPPH (0.1 mmol).

The mixture was shaken thoroughly and kept in the dark environment for 30 minutes, and the absorbance was recorded at 517 nm against a blank using ultra violet-visible spectrophotometer. Rutin & Quercetin was used as the reference standard. The total antioxidant power of Ru-Qr nanoparticles was expressed as percentage of scavenging of DPPH radicals, the % DPPH scavenging (antioxidant power) was calculated by using the following formula:

$$A_0 - A_1) \times 100/A_0 \qquad (1)$$

Where A_0 = absorbance of the control;
A_1 = absorbance of the sample.

In vitro drug releasing capacity

The *in vitro* drug releasing capacity of nanoparticles was measured by previously described method with some modifications [19]. First, free drug (Ru-Qr) was separated from nanoparticles by passing through sephadex dialysis column and then subjected to centrifugation. The separated particles dissolving 2 mL of PBS (0.01M, pH 7.4), then suspension was equally divided in two tubes containing 1 mL each (as the experiment was performed in duplicate) and kept in a shaker at 37°C at 150 rpm. Samples were withdrawn at definite time intervals and replaced with same volume of fresh phosphate buffer solution pH 7.4. The collected supernatant was lyophilized and dissolved in 1 mL of DMSO/acetone. The solution was centrifuged at 14,000 rpm for 10 minutes at 25°C to collect the drug in the supernatant. It was then analyzed for drug contents by spectrophotometrically. Rutin & Quercetin was used as the reference standard.

$$\%DRC = (A_0 - A_1) \times 100/A_0 \qquad (2)$$

Where A_0 = absorbance of the control;
A_1 = absorbance of the sample.

Particle size, Polydispersity index and Zeta potential measurements

The average particle size, polydispersity index and zeta potential of Ru-Qr loaded nanoparticles were measured by dynamic laser scattering and laser doppler anemometry using Zetasizer Nano ZS (Malvern Instruments, Malvern, UK). Measurements were performed in a dilute suspension of void nanoparticles; Ru-Qr loaded nanoparticles were prepared in distilled water, sonicated on an ice-bath for 30 seconds and subjected to particle size, polydispersity index and zeta potential measurements separately. All measurements were performed triplicates.

Selection of relevant variables and experimental design

In this context of our experimental design, the parameters involved in the preparation of Ru-Qr dual drug loaded keratin nanoparticles was optimized through response surface methodology. A central composite design was used to identify the optimum combination of parameters for preparation of dual drug loaded keratin nanoparticles. The independent variables, namely surfactant (X_1: SDS [1], Sodium Lauryl Sulphate [2], Tween-20 [3]), organic solvents (X_2: acetone [1] methanol [2], chloroform [3],) and temperature (X_3:10-40 C) and the dependent variables drug releasing capacity, average particle size, polydispersity index, total antioxidant power, and zeta potential were selected for optimum preparation of Ru-Qr dual drug loaded nanoparticles. The independent variables were coded at five levels (-1.682, -1, 0, +1and +1.682) was presented in **Table 1**. All of the experiments were carried out in triplicates and the experimental results were expressed as mean ±standard deviations, and statistical analysis was performed by design expert statistical software (version 8.0.7.1, Stat-Ease, Inc., Minneapolis, MN, USA). The Central composite design was comprised of 20 runs with 8 factorial points, 6 axial points at a distance of ± 1.682 from the central points as shown in **Table 2**. According to the experimental data, and to develop second order polynomial equation for calculate the response surface analysis as shown below:

$$Y = S_0 + \sum_{i=1}^{3} S_i X_i + \sum_{i=1}^{3} S_{ii} X_i^2 + \sum_{i=1}^{2} \sum_{j=i+1}^{3} S_{ij} X_i X_j + V \quad (3)$$

In this study, equation (3) shall be rewritten by applying the values of three variables

$$Y = S_0 + S_1 X_1 + S_2 X_2 + S_3 X_3 + S_{12} X_1 X_2 + S_{13} X_1 X_3 + S_{23} X_2 X_3 + S_{11} X_1^2 + S_{22} X_2^2 + S_{33} X_3^2 \quad (4)$$

Where Y is the dependent variables (drug releasing capacity, average particle size, polydispersity index, total antioxidant power, and zeta potential), $\hat{a}_0$ is the model constant, S_i, S_{ii}, and S_{ij} are the model coefficients, X_i and X_j are coded value of the independent variables, and V is the error. Confirmatory experiments were carried out to validate the statistical experimental analysis. Optimized Ru-Qr nanoparticles size, shape, biomolecules will be analyzed by SEM-EDS, XRD, and FTIR.

SEM-EDS

The scanning electron microscopy (SEM) analysis was carried by a Carl Zeiss EVO-18 electron microscope. For SEM imaging to visualize the morphological size and shape of the optimized dual drug loaded keratin nanoparticles, a sample of a nanoparticles solution was placed on a carbon strip attached to a SEM brass, extra solution was detached using blotting paper and then allowed to dry by putting it under a mercury lamp for 5 min.

The elemental compositions of dual drug loaded keratin nanoparticles were obtained using BRUKER EDS-(QUANTAX 200-XFLASH) SDD (Silicon Drift Detector) by Variable Pressure mode, at acceleration voltage of 20 KeV.

FTIR

The Fourier transform infrared spectra were recorded using IR Tracer-100 Shimadzu, FTIR, and using the spectral range 4000-400cm^{-1} with resolution of 4cm^{-1}. A small amount (=1mg) of finely powdered lyophilized optimized dual drug loaded keratin nanoparticles was mixed with IR grade Potassium bromide (KBr) to obtain a round disc (with help of hydraulic press) suitable for FTIR measurement.

XRD

The crystalline and the lattice characteristics of the synthesized optimized dual drug loaded keratin nanoparticles were measured by powder X-ray diffraction analysis. The XRD measurement was carried out on thoroughly dried thin films of the purified lyophilized optimized dual drug loaded

keratin nanoparticles powder, and lyophilized powder was dirtied on a glass slab on a D8 Advance ECO XRD Systems with SSD160 1D Detector-Bruker XRD 6000 instrument operated at a voltage of 20 keV and a current of 30mA with CuKг 1 radiation (}=0.1542) in a „ - 2 theta (degree) configuration.

Statistical data analysis

The experimental data collected from response surface methodology was analyzed using Design Expert (version 8.0.7.1, Stat-Ease, Inc, Minneapolis, MN, USA) statistical software. All the results were expressed as the mean ± standard deviation. The optimal experimental parameters were analyzed by one way analysis of variance (ANOVA), three dimensional (3D) response surfaces and contour plots. The software generated regression coefficient for each of the independent variables and the significance was determined using the p value generated through t-test.

RESULTS AND DISCUSSIONS

In the present research work, we investigated preparation, and characterization of Ru-Qr dual drug loaded keratin nanoparticles, and also analyzing the suitable parameters for preparing optimal nanoparticles. The amount of keratin present in the extracted human hair was estimated by using Bradford method. The purified human hair extract was contains 92.5 % keratin as compared to the analytical grade keratin (obtained from Himedia Laboratories, Mumbai, India).

In this study, the development of optimization using response surface methodology, the suitable independent parameters for preparing optimal nanoparticles namely, temperature, surfactant and solvent and the dependent parameters namely, drug releasing capacity, average particle size, total anti-oxidant power, zeta potential, polydispersity index were investigated. In this condition, to obtain suitable working range for each of the parameters and to preliminary investigation was done for critical factors and further utilized for optimization of each factor using response surface methodology (RSM). In RSM, 20 sets of experiments have been conducted by using CCD, predicted and experimental results are presented in Table 2. Results indicate that among the selected independent variables, temperature has a significant effect on drug releasing capacity, average particle size, total anti-oxidant power, zeta potential, and polydispersity index. It has been observed that the maximum drug releasing capacity was 98.3 mg and the minimum average particle size was 125 mm at 40°C. The maximum antioxidant power was recorded to be 98.68%, zeta potential 28.09, polydispersity index 0.54 was obtained at 40°C when surfactant and solvents were constant. The optimum point of response variables were attained under the same conditions.

Fitting the models

The experiments were performed within the parameters and their range as shown in Table 1. Ru-Qr dual drug loaded keratin nanoparticles was prepared solid dispersion method. The prepared nanoparticles was tested on drug releasing capacity, average particle size, total anti-oxidant power, zeta potential, polydispersity index, and their experimental and predicted results were presented in Table 2.

The responses were fitted to a second order polynomial equation and Table 3 shows the results of fitting quadratic models with the data. The experimental models were validated by ANOVA and to find coefficients of the individual responses and the regression coefficients of the obtained equations. The significance of the responses was monitored by F test and p at 95 % confidence level. The experimental variables would be more suitable and significant if the F-value becomes greater and the p-value becomes smaller [20]. The p-values were used as an important tool to check the significance and adequacy of the interactions of the variables. A p-value less than 0.05 indicated that the coefficient was statistically significant.

The fitting of the model was confirmed by the determination of multiple regression coefficients (R^2) and the significance of lack-of-fit. The second–order polynomial equation for the fitted quadratic models for drug releasing capacity, average particle size, total anti-oxidant power, zeta potential, polydispersity index in coded variables are given in equations.

$$DRC = 91.23 + 2.80X_1 - 0.48X_2 - 0.38X_3 - 0.35X_1X_2 - 0.25X_1X_3 + 0.15X_2X_3 + 0.22X_1^2 + 1.44X_2^2 + 1.56X_3^2 \quad (5)$$

$$APS = 52.21 - 4.33X_1 + 2.15X_2 + 1.74X_3 + 2.37X_1X_2 + 2.38X_1X_3 - 4.63X_2X_3 - 0.33X_1^2 - 2.6X_2^2 - 3.86X_3^2 \quad (6)$$

$$TAP = 85.66 + 4.92X_1 - 1.45X_2 - 0.72X_3 \quad (7)$$

ZP $=-12.16+6.70X_1-1.04\ X_2+0.015X_3-1.14\ X_1X_2+$
$0.81\ X_1X_3+4.01\ X_2X_3+2.55\ X_1^2+2.32\ X_2^2+3.31X_3^2$ (8)

PI $=1.02-0.10X_1+0.070\ X_2+1.631E\text{-}003\ X_3$
$+0.034\ X_1X_2+0.026\ X_1X_3-0.069X_2X_3$ (9)
$-3.369E\text{-}004X_1^2-0.037\ X_2^2-0.12\ X_3^2$

Table 1. Experimental parameters and range of coded and actual parameters of central composite design (CCD)

Independent variables (x_j)	Symbols	Factor levels				
		-1.682	-1	0	+1	+1.682
Temperature(°C)	X_1	-0.23	10	25	40	50.23
Surfactant (5 mg)	X_2	SLS:SDS	SLS	SDS	TWEEN-20	SDS:TWEEN-20
Solvent (90 %)	X_3	Ace:meth	Acetone	Methanol	Chloroform	Meth:chlo

Table 2. Central Composite Design with experimental responses and predicted responses

Sl. No	Temp. (°C)	*Surfactant (5 mg)	*Organic solvent (90 %)	Experimental Value (Y_1)[a]					Predicted Value (Y_2)				
				Drug releasing capacity (%)	Average particle size (nm)	Total anti-oxidant power (%)	Zeta potential (mV)	Polydispersity index	Drug releasing capacity (%)	Average particle size (nm)	Total anti-oxidant power (%)	Zeta potential (mV)	Polydispersity index
1	10	3	1	91.8	154	87.24	-15.08	1.01	91.493	54.761	80.011	-13.803	1.09
2	10	3	3	91.8	146	80.05	-5.28	0.95	91.532	144.235	78.564	-7.35	0.9
3	40	3	1	96.2	146	90.25	14.78	0.97	96.897	146.094	89.854	10.90	0.9
4	40	1	3	96.7	145	91.32	25.06	0.86	97.297	145.262	91.3	19.68	0.74
5	25	2	3.681793	94.9	144	87.07	-6.02	0.81	94.99	144.21	84.43	-2.78	0.69
6	40	1	1	98.3	125	98.68	28.09	0.54	98.858	127.78	92.75	24.60	0.55
7	0.22689	2	2	86.5	158	79.87	-18.92	1.34	88.644	156.212	80.737	-16.309	1.11
8	25	2	2	90.4	153	83.56	-12.07	0.92	91.228	152.208	85.659	-12.158	1.01
9	50.22689	2	2	97.6	146	94.67	26.08	0.65	96.555	143.99	93.93	28.12	0.84
10	25	2	2	90.4	152	85.32	-11.98	1.05	91.22	152.2	85.65	-12.15	1.01
11	25	0.318207	2	96.5	143	89.96	-8.06	0.87	96.146	141.06	88.1	-3.77	0.79
12	25	2	2	90.3	150	82.26	-12.2	1.03	91.22	152.2	85.65	-12.15	1.017
13	25	2	2	91.5	151	83.01	-12.08	1.03	91.22	152.2	85.65	-12.15	1.017
14	40	3	3	95.8	144	88.45	24.56	1.01	95.936	145.068	88.406	13.94	0.81
15	25	2	2	92.4	155	84.26	-12.06	1.03	91.22	152.2	85.65	-12.15	1.017
16	25	3.681793	2	94.5	148	80.03	-6.08	0.91	94.47	148.41	83.22	-7.37	1.02
17	25	2	0.318207	96.8	140	84.04	-2.48	0.8	96.33	138.23	86.88	-2.71	0.67
18	10	1	3	91.9	153	80.23	-13.04	0.93	91.49	153.92	81.46	-15.58	0.96
19	25	2	2	92.3	152	84.05	-12.06	1.05	91.22	152.2	85.65	-12.15	1.017
20	10	1	1	91.9	146	78.86	-3.09	0.72	92.05	145.95	82.91	-5.96	0.88

[a] All the experiments were repeated three times
*Surfactant: 1-SDS, 2-Sodium Lauryl Sulphate, 3-Tween-20, 0.318207-SDS: SLS, 3.681793-SDS: Tween-20
*Solvent: 1-Acetone, 2-Methanol, 3-Chloroform, 0.318207-acetone: methanol, 3.681793-Acetone: chloroform

Analysis of the model
Drug releasing capacity

It can be seen from Table 3, it may be incidental that the variables with linear term (X_1, temperature), and quadratic term (X_2^2, X_3^2) were significantly ($p<0.05$) involved in the preparation of protein nanoparticles and their largest effect on drug releasing capacity. The involvement of surfactant and solvent is relatively less in the drug releasing capacity of protein nanoparticles. The maximum drug releasing capacity 98.3 was obtained at temperature 40ÚC, surfactant (SDS), and solvent (acetone). The correlation coefficient (R^2) of the predicted model regarding drug releasing capacity of nanoparticles was 0.9544 with p-value of lack of fit was 0.639. In addition, the predicted data against experimental data gave a higher R^2 value of 0.9544 compared to RSM's R^2 value of 0.8175 (Fig. 1 A). The high values of regression coefficient ($R^2 >> 0.8$) a good fit. Equation [5] shows the relationship between drug releasing capacity and involvement of independent parameters for optimum nanoparticles preparation.

Table 3: Analysis of variance (ANOVA) for the quadratic polynomial mode

Source	Sum of Squares	DF[a]	Mean Square	F value[b]	p-value[c]
Drug Releasing Capacity[d]					
Model	173.14	9	19.24	23.24	< 0.0001
X_1	107.23	1	107.23	129.51	< 0.0001
X_2	3.15	1	3.15	3.18	0.0795
X_3	1.98	1	1.98	2.39	0.1534
$X_1 X_2$	0.98	1	0.98	1.18	0.3021
$X_1 X_3$	0.50	1	0.50	0.60	0.4551
$X_2 X_3$	0.18	1	0.18	0.22	0.6510
X_1^2	0.68	1	0.68	0.83	0.3848
X_2^2	29.78	1	29.78	35.97	0.0001
X_3^2	35.13	1	35.13	42.43	< 0.0001
Residual	8.28	10	0.83		
Lack of Fit	3.45	5	0.69	0.71	0.6392
Pure Error	4.83	5	0.97		
Cor Total	181.42	19			
Average Particles Size[e]					
Model	911.89	9	101.32	25.94	< 0.0001
X_1	256.46	1	256.46	65.65	< 0.0001
X_2	63.33	1	63.33	16.21	0.0024
X_3	41.22	1	41.22	10.55	0.0087
$X_1 X_2$	45.12	1	45.12	11.55	
$X_1 X_3$	45.12	1	45.12	11.55	
$X_2 X_3$	171.13	1	171.13	43.81	
X_1^2	1.56	1	1.56	0.4	
X_2^2	99.48	1	99.48	25.47	
X_3^2	215.26	1	215.26	55.11	
Residual	39.06	10	3.91		
Lack of Fit	24.23	5	4.85	1.63	0.3017
Pure Error	14.83	5	2.97		
Cor Total	950.95	19			
Total Antioxidant Power[f]					
Model	366.63	3	122.21	11.46	0.0003
X_1	330.77	1	330.77	31.02	< 0.0001
X_2	28.71	1	28.71	2.69	0.1204
X_3	7.15	1	7.15	0.67	0.4248

Source	Sum of Squares	DF[a]	Mean Square	F value[b]	p-value[c]
Total Antioxidant Power[f] (Continued)					
Residual	170.64	16	10.66		
Lack of Fit	165.02	11	15	13.35	0.0051
Pure Error	5.62	5	1.12		
Cor Total	537.27	19			
Zeta Potential[g]					
Model	1048.87	9	116.54	16.57	< 0.0001
X_1	612.57	1	612.57	87.1	< 0.0001
X_2	14.91	1	14.91	2.12	0.176
X_3	3.12E-03	1	3.12E-03	4.44E-04	0.9836
$X_1 X_2$	10.44	1	10.44	1.48	0.251
$X_1 X_3$	5.22	1	5.22	0.74	0.4093
$X_2 X_3$	128.96	1	128.96	18.34	0.0016
X_1^2	93.48	1	93.48	13.29	0.0045
X_2^2	77.37	1	77.37	11	0.0078
X_3^2	158.28	1	158.28	22.51	0.0008
Residual	70.33	10	7.03		
Lack of Fit	70.3	5	14.06	2795.32	< 0.0001
Pure Error	0.025	5	5.03E-03		
Cor Total	1119.2	19			
Polydispersity Index[h]					
Model	0.48	9	0.054	2.36	0.0982
X_1	0.14	1	0.14	6.24	0.0316
X_2	0.067	1	0.067	2.96	0.1163
X_3	3.64E-05	1	3.64E-05	1.60E-03	0.9689
$X_1 X_2$	9.11E-03	1	9.11E-03	0.4	0.5405
$X_1 X_3$	5.51E-03	1	5.51E-03	0.24	0.6327
$X_2 X_3$	0.038	1	0.038	1.67	0.2258
X_1^2	1.64E-06	1	1.64E-06	7.21E-05	0.9934
X_2^2	0.02	1	0.02	0.89	0.3674
X_3^2	0.21	1	0.21	9.23	0.0125
Residual	0.23	10	0.023		
Lack of Fit	0.21	5	0.043	17.78	0.0034
Pure Error	0.012	5	2.42E-03		
Cor Total	0.71	19			

[a]Degrees of freedom; [b]Test for comparing model variance with residual (error) variance; [c]Probability of seeing the observed F-value if the null hypothesis is true
[d]The coefficient of determination (R^2) of the model was 0.9544; [e]The coefficient of determination (R^2) of the model was 0.9589
[f]The coefficient of determination (R^2) of the model was 0.6824; [g]The coefficient of determination (R^2) of the model was 0.9372
[h]The coefficient of determination (R^2) of the model was 0.6803

Fig 1 B & C 3-D representation of the response surfaces and the contours plot showing the significant involvement between independent variables such as surfactant and temperature by the effect of maximum the drug releasing capacity of nanoparticles preparation.

Results in Table 2 shows that maximum drug releasing capacity of nanoparticles was obtained at temperature 40°C, surfactant (SDS] and solvent (acetone).

Average particle size

The response surface analysis in Table 3 and model equation [6] shows the linear term of temperature (X_1), surfactant (X_2) and solvent (X_3) has significant involvement in the preparation of minimal particles sized keratin nanoparticles. In Table 3 shows that the effects of temperature (X_1), surfactant (X_2) and solvent (X_3) are significant (p< 0.05). All other terms are not significant (P>0.05). The response surface analysis of average particles size also demonstrated high regression coefficient value R^2 =0.9589 and p-value for lack of fit was 0.3017. In addition, the predicted data against experimental data gave a higher R^2 value of 0.9589 compared to RSM's R^2 value of 0.7741 (Fig. 2A). In the consequence of the model equation (6) showing the relationship between linear terms, quadratic terms and interaction terms of minimal particles sized keratin nanoparticles.

Total antioxidant power

The polynomial equation and ANOVA table, it is evident that the linear term of temperature (X_1) has involved in the preparation of nanoparticles and significant effect (p<0.05) for antioxidant effects. Although the regression coefficient value (R^2) of the models was 0.6824, p-value for lack of fit was 0.0051. In addition, the predicted data against experimental data gave a higher R^2 value of 0.6824 compared to RSM's R^2 value of 0.4481 (Fig. 3A). In consequence of equation (7) showing the relationship between total antioxidant and preparation parameters may be considered to be valid in the present range of operating parameters.

Fig 3B and C illustrates the involvement of temperature and surfactant for preparation of keratin nanoparticles and their antioxidant activity. Results in Table 2 shows that maximum antioxidant activity of nanoparticles was obtained at temperature 40°C, surfactant (SDS) and solvent (acetone).
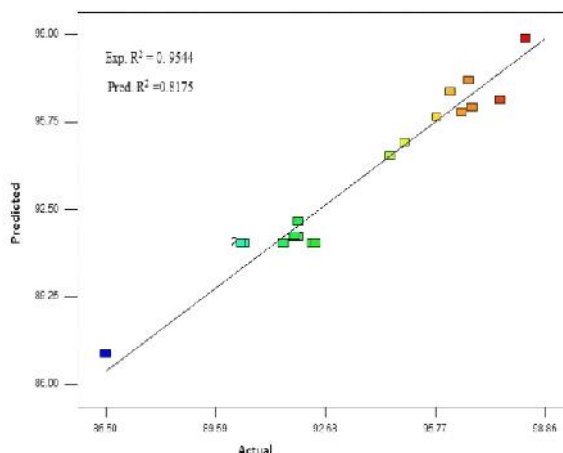

Fig. 1A. Relationship between experimental and predicted value of temperature and surfactant by drug releasing capacity of nanoparticles
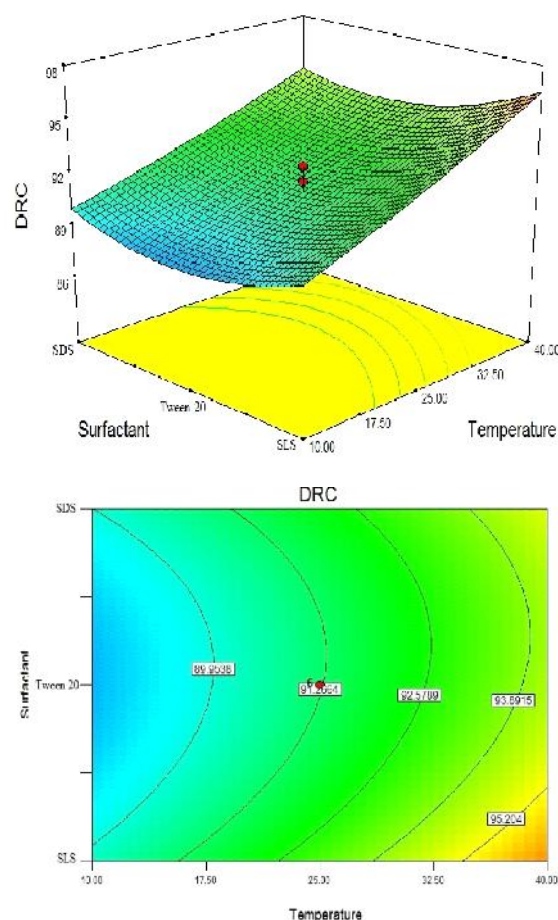

Fig .1B and 1C. Response surface and contour plot showing the combined effects of temperature and surfactant for preparation of nanoparticles and highest drug releasing capacity
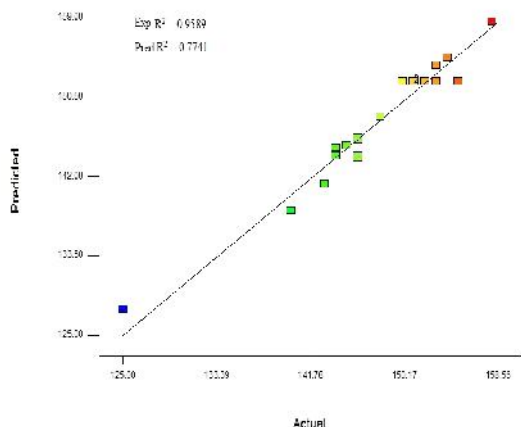
Fig .2A. Relationship between experimental and predicted value of temperature and surfactant by average particles size of nanoparticles
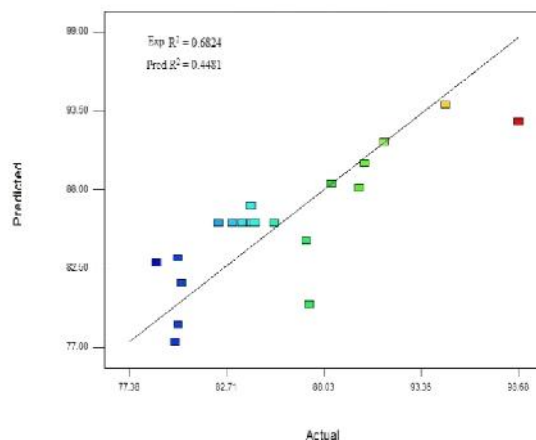

Fig. 3A. Relationship between experimental and predicted value of temperature and surfactant by total antioxidant of nanoparticles
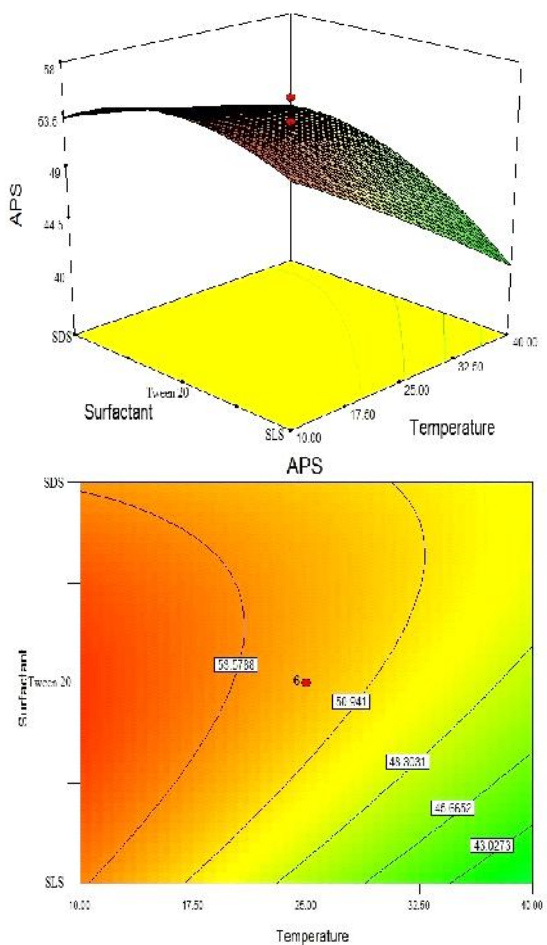

Fig .2B and 2C.Response surface and contour plot showing the combined effects of temperature and surfactant for preparation of nanoparticles and minimal particles size
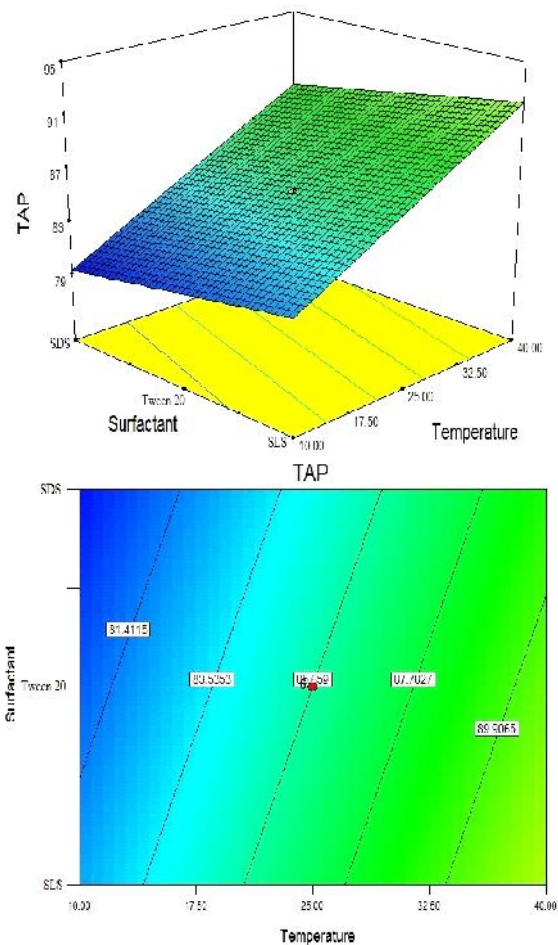
Fig. 3B and 3C. Response surface and contour plot showing the combined effects of temperature and surfactant for preparation of nanoparticles and antioxidant power

261

Zeta potential

Zeta potential is a key indicator for the determination of stability of the nanoparticles in colloidal system. The magnitude of the zeta potential indicates the electrostatic repulsion between similar charged particles in dispersion. Higher number of either positive or negative charge repels each other which inturn prevents the aggregation. Particle charge was quantified and expressed as zeta potential. The effects of temperature, surfactant and solvent on nanoparticles have been examined thoroughly. From that response model it can be showed that temperature has influenced significantly ($p < 0.05$) on zeta potential of the nanoparticles. The p-value for lack of fit was also found to be significant ($p < 0.0001$). The coefficient of regression (R^2) of the model was 0.9372. Fig. 4A shows that, the predicted data against experimental data gave a higher R^2 value of 0.9372 compared to RSM's R^2 value of 0.5142. The response surfaces and the contour plots indicates the optimum value of zeta potential as 28.09mV when the temperature was 40 C. Analysis of the data showed that the best model to predict the optimal responses for zeta potential was quadratic. Fig 4B and C represents the involvement of temperature and surfactant for preparation of keratin nanoparticles and their effective zeta potential. Results in Table 2 shows that maximum zeta potential of nanoparticles was obtained at temperature 40°C, surfactant (SDS) and solvent (acetone).

Polydispersity index

Analysis of the contour plot and response plot of optimization models revealed that neither of the independent factors (temperature, solvent, surfactant) has significant effect on polydispersity index. The lack of fit with p-value 0.0034 is found to be significant.

The experimental values of the nanoparticles are prepared within the optimum range and are very close to the predicted values.

The response surface analysis of polydispersity index also demonstrated high regression coefficient value $R^2 = 0.6803$.

Fig 5A shows that, the predicted data against experimental data gave a higher R^2 value of 0.6803 compared to RSM's R^2 value of 0.3926. In consequence of the model equation (8) showing the relationship between polydispersity index and nanoparticles preparation parameters is valid.
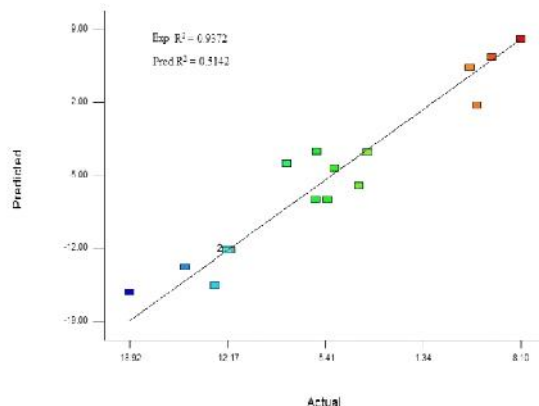

Fig. 4A. Relationship between experimental and predicted value of temperature and surfactant by zeta potential of nanoparticles
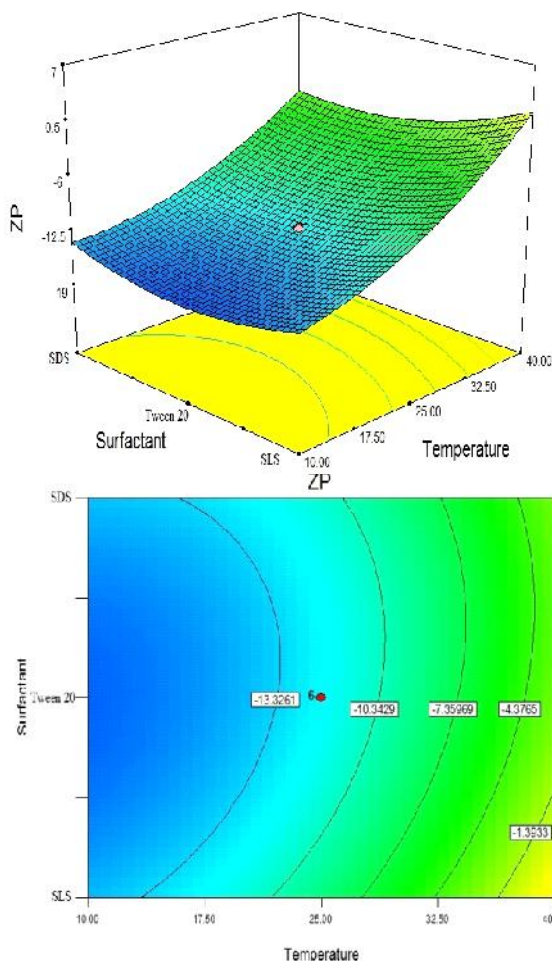

Fig. 4B and 4C. Response surface and contour plot showing the combined effects of temperature and surfactant for preparation of nanoparticles and zeta potential
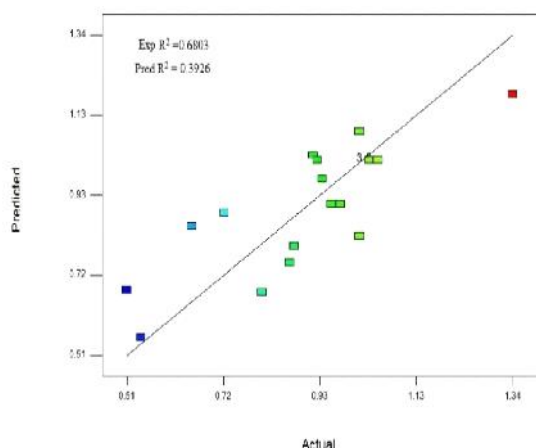
Fig. 5A. Relationship between experimental and predicted value of temperature and surfactant by polydispersity index of nanoparticles
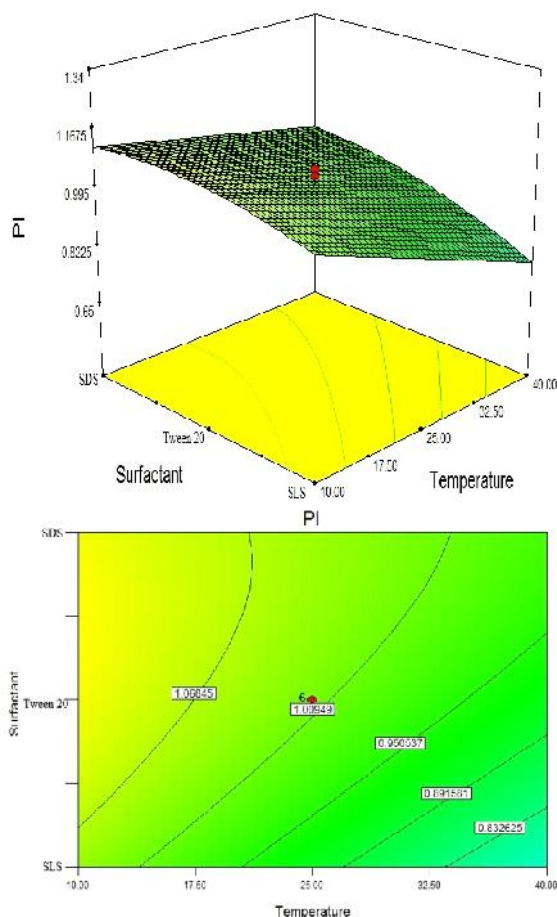

Fig. 5B and 5C. Response surface and contour plot showing the combined effects of temperature and surfactant for preparation of nanoparticles and polydispersity index

Fig 5A and B represents the involvement of temperature and surfactant for preparation of keratin nanoparticles and their effective polydispersity index.

Table 2 shows that effective polydispersity of nanoparticles was obtained at temperature 40°C, surfactant (SDS) and solvent (acetone).

Verification of the model

The suitability of the verification experimental values was tested by using the selected optimal conditions to find the reliability of the optimization result. Table 4 shows the verification experiment under optimum conditions based on each individual response with predicted and experimental values. The verification experiment was executed under optimum conditions based combinations of responses and small deviation was observed as compared to predicted values. Optimal conditions based on combination of responses were: temperature: 35-45 C, surfactant: SDS and solvent of acetone. Under this, optimum operating conditions for drug releasing capacity, average particles size, total antioxidant power, zeta potential, polydispersity index were 94.3-98.3, 123-125, 93.68-95.68, 26.04-28.05, 0.50-0.54 respectively.

This model implied a good fit between experimental value and those predicted by the regression model.

Characterization of optimized nanoparticles
SEM-EDX analysis

SEM images shown in Fig. 6, the morphological characteristics of optimized Ru-Qr dual drug loaded keratin nanoparticles.

The overall morphological shapes of the Ru-Qr dual drug loaded keratin nanoparticles were spherical.

The average sizes of the of Ru-Qr dual drug loaded keratin nanoparticles were 18–25 nm.

EDX analysis of Ru-Qr dual drug loaded keratin nanoparticles presented in Fig. 7, showed the strong signals of metals present in the protein based nanoparticles. EDX analyses suggested that keratin engulfed Ru-Qr were strongly responsible for the stability of the biosynthesized Ru-Qr dual drug loaded keratin nanoparticles.

FTIR analysis

In the qualitative determination of potential functional biomolecules involvement in preparation

Table 4. Verification of experimental and predicted values under optimum conditions based on combination of responses

	Coded Variable levels			Experimental value (Y₁)ᵃ					Predicted value (Y₂)				
Run	Temp. (°C)	*Surfactant (5 mg)	*Organic solvent (90 %)	Drug releasing capacity (%)	Average particle size (nm)	Total anti-oxidant power (%)	Zeta potential (mV)	Polydispersity index	Drug releasing capacity (%)	Average particle size (nm)	Total anti-oxidant power (%)	Zeta potential (mV)	Polydispersity index
1	35	1	1	94.3	123	93.68	26.04	0.50	96.272	129.199	91.815	16.708	0.60
2	40	1	1	97.8	125	97.00	28.05	0.52	97.347	126.07	94.35	24.34	0.53
3	45	1	1	98.3	125	95.68	27.06	0.54	98.46	122.94	96.89	33.21	0.468

ᵃ All the experiments were repeated three times
*Surfactant: 1-SDS, 2-Sodium lauryl Sulphate, 3-Tween-20, 0.318207-SDS: SLS, 3.681793-SDS: Tween-20
*Solvent: 1-Acetone, 2-Methanol, 3-Chloroform, 0.318207-acetone: methanol, 3.681793-Acetone: chloroform
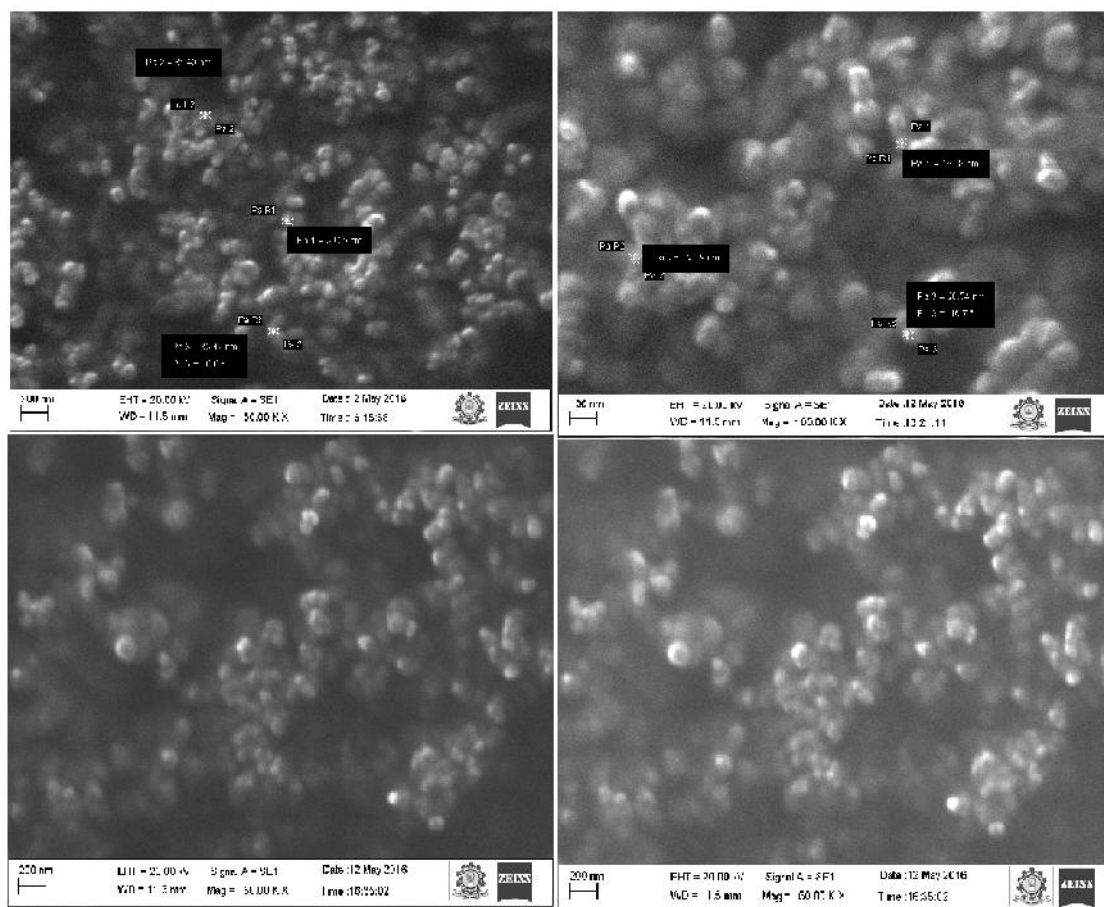

Fig. 6. SEM images of optimized Ru-Qr dual drug loaded keratin nanoparticles

of dual drug loaded keratin nanoparticles were recorded by FTIR spectra.

The spectra of dual drug loaded human hair keratin nanoparticles were shown in Fig. 8.

The analysis of FTIR spectra of lyophilized Ru-Qr drug loaded keratin nanoparticles showed peaks (Vmax) at 3741, 3417 cm⁻¹ indicating the presence of strong O-H bonding of carboxyl groups and strong N–H stretching of secondary amides; 2881 cm⁻¹ indicating the presence of –CH₂ stretching of aliphatic groups; 2347, 2065 cm⁻¹ representing alkynyl C–H bonding, alkynyl C≡C stretching; 1732, 1662 cm⁻¹
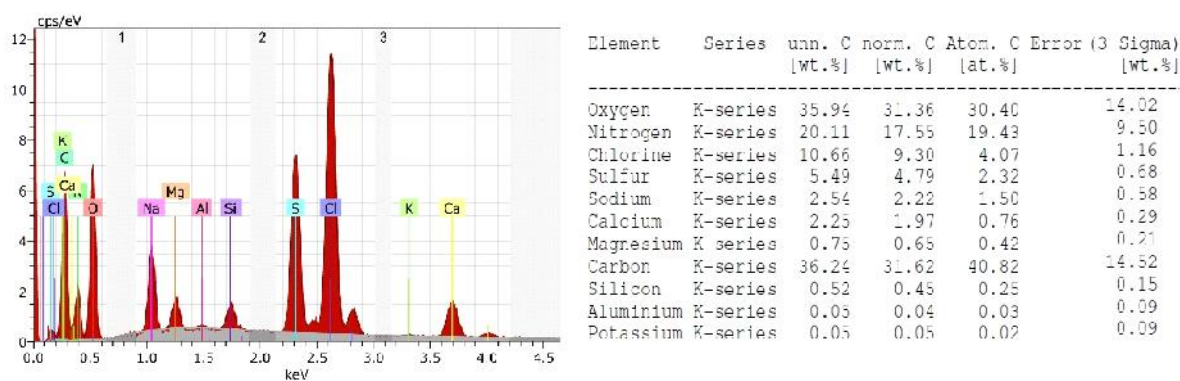
Element	Series	unn. C [wt.%]	norm. C [wt.%]	Atom. C [at.%]	Error (3 Sigma) [wt.%]
Oxygen	K-series	35.94	31.36	30.40	14.02
Nitrogen	K-series	20.11	17.55	19.43	9.50
Chlorine	K-series	10.66	9.30	4.07	1.16
Sulfur	K-series	5.49	4.79	2.32	0.68
Sodium	K-series	2.54	2.22	1.50	0.58
Calcium	K-series	2.25	1.97	0.76	0.29
Magnesium	K-series	0.75	0.65	0.42	0.21
Carbon	K-series	36.24	31.62	40.82	14.52
Silicon	K-series	0.52	0.45	0.25	0.15
Aluminium	K-series	0.05	0.04	0.03	0.09
Potassium	K-series	0.05	0.05	0.02	0.09

Fig. 7. EDX-pattern of optimized Ru-Qr dual drug loaded keratin nanoparticles
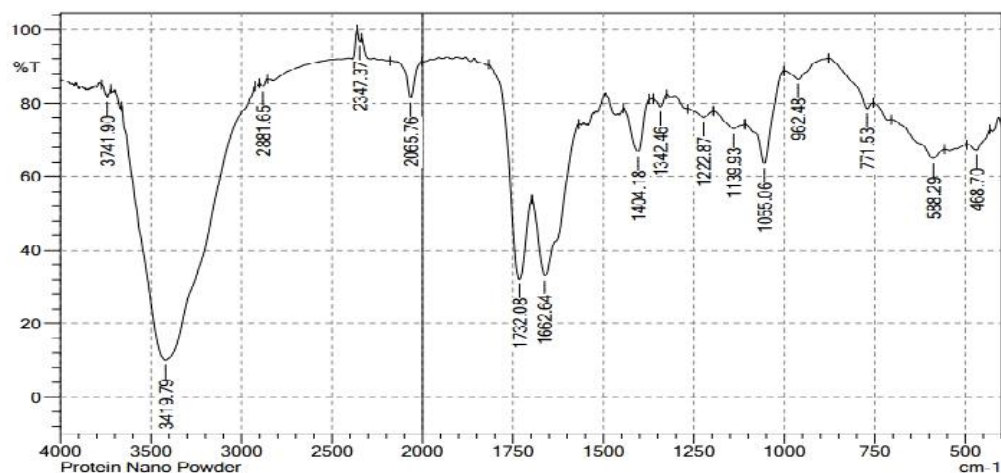
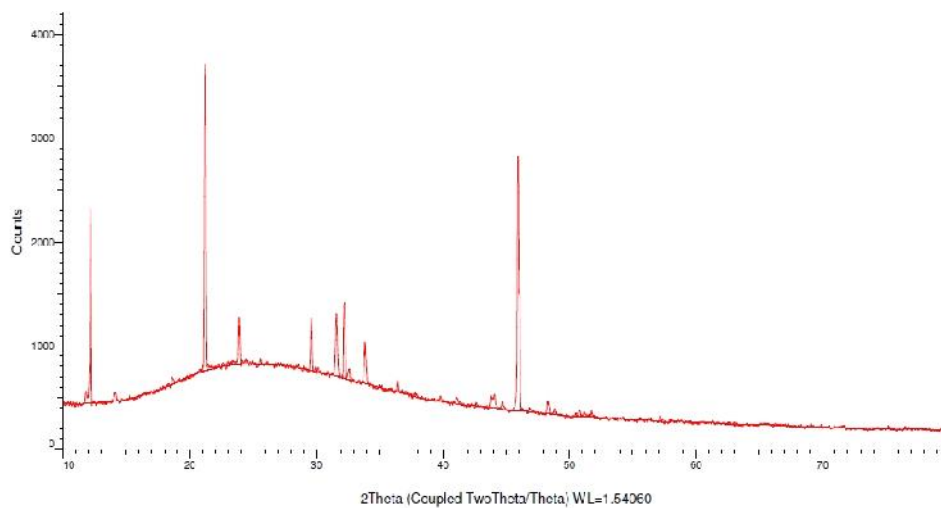Fig. 8. FTIR spectra of optimized Ru-Qr dual drug loaded keratin nanoparticles

Fig. 9. XRD pattern of optimized Ru-Qr dual drug loaded keratin nanoparticles lyophilized powder

265

representing the bonds with C–N stretching, = N–H deformation, COO– anions and C = C aromatic conjugates; 1404 cm^{-1} indicating C = O groups from aromatic rings having conjugation and 1342, 1222, 1139, 1055 cm^{-1} showing bending vibrations of C–OH alcoholic group and C–O single bond vibrations of ether linkages. Based on the previous literature, functional groups C–O, C–OH, C = O, NH and COO from amino acids and proteins has strong affinity to bind proteins to produce highly stable nanoparticles [21].

XRD analysis

Physical nature of the Ru-Qr dual drug loaded keratin nanoparticles was characterized by XRD technique and the corresponding XRD-diffractogram presented in Fig. 9 was analyzed. Diffraction peaks observed at 2è = 12, 21, 23, 27, 33, and 46 suggesting that they are highly crystalline nature. The size of the Ru-Qr dual drug loaded keratin nanoparticles was calculated by Debye–Scherrer's equation:

$$D = \frac{k\lambda}{\beta s \cos\theta} \qquad (10)$$

Where, D is crystallite size, K is size-dependent Debye–Scherrer's constant (0.94 for spherical particles), λ is incident X-radiation wavelength (1.548 Å), and βs is full peak width at half maxima. Average size of the synthesized Ru-Qr dual drug loaded keratin nanoparticles is calculated to be 20 nm.

CONCLUSION

In the present work, preparation of Ru-Qr dual drug loaded keratin nanoparticles for biological applications, and preparative parameters were developed, and validated. Keratin is extracted and purified from waste human hair. RSM results showed the independent parameters (temperature, surfactant, and solvent), and quadratic terms (temperature and surfactant), and the interaction terms (temperature, surfactant, and solvent) involving significant effects on the yield of minimal sized, maximum drugs engulfed nanoparticles. Consequently all three parameters have significant contribution for the effective preparation of dual drug loaded nanoparticles. The validity of the model was judged by fitting the values of the observed experimental values and by carrying out experiments using the predicted values. Nanotechnology based drug delivery system offers enhanced therapeutic efficacy and reduce undesirable adverse side effects associated with conventional drug, introduce new classes of therapeutics and encourage the re-investigation of pharmaceutically suboptimal but biologically active new molecular entities that were previously considered undevelopable.

AUTHORS' CONTRIBUTIONS

All the authors contributed equally in the preparation of this research article.

CONFLICT OF INTEREST STATEMENT

The authors declare no competing financial interest.

REFERENCES

1. Heller A. Integrated medical feedback systems for drug delivery. AlChE J. 2005; 51(4): 1054-1066.
2. Roszek B, De Jong WH, Geertsma RE. Nanotechnology in medical applications: state-of-the-art in materials and devices. RIVM report. 265001001/2005.
3. Singh R, Lilard JW. Nanoparticle-based targeted drug delivery. Exp Mol Pathol. 2009; 86(3): 215-223.
4. Selvaraj. K, Chowdhury. R, Bhattacharjee. C. A green chemistry approach for the synthesis and characterization of gold nanoparticles stabilized with methanol extract of *Azolla microphylla* and their enhanced antioxidant activity. Front Mat Sci. 2014; 8(2): 123–135.
5. Liechty WB, Kryscio DR, Brandon V. Slaughter, Peppas NA. Polymers for drug delivery systems. Annu Rev Chem Biomol Eng. 2010; 1: 149-173.
6. Lohcharoenkal W, Wang L, Chen YC, Rojanasakul Y. Protein nanoparticles as drug delivery carriers for cancer therapy. Biomed Res Int. 2014; 2014: 1-12.

7. Elzoghby AO, El-fotoh WS, Elgindy NA. Casein-based formulations as promising controlled release drug delivery systems. J control release. 2011; 153:206-216.

8. Nie S. Understanding and overcoming major barriers in cancer Nanomedicine. Nanomedicine (Lond). 2010; 5(4): 523-528.

9. Maham A, Tang Z, Wu H, Wang J, Lin Y. Protein-based Nanomedicine platforms for drug delivery. Small 2009; 5(15): 1706-1721.

10. Kakkar P, Madhan B, Shanmugam S. Extraction and characterization of keratin from bovine hoof: A potential material for biomedical applications. Springer plus. 2014; 3: 596.

11. Feughelmann M. Keratin. Encyclopedia of polymer science and engineering. New York, Wiley.1985.

12. Marshall RC, Orwin DF, Gillespie JM. Structure and biochemistry of mammalian hard keratin. Electron Microsc Rev. 1991; 4(1): 47-83.

13. Parani M, Lokhande G, Singh A, Gaharwar AK. Engineered Nanomaterials for infection control and healing acute and chronic wounds. ACS Appl Mater Interfaces. 2016; 8(16): 10049-10069.

14. Chaudhury K, Kumar V, Kandasamy J, Roychoudhury S. Regenerative nanomedicine: current perspectives and future directions. Int J Nanomed. 2014; 9: 4153-4167.

15. Scarano W, de souza P, Stenzel MH. Dual-drug delivery of curcumin and platinum drug in polymeric micelles enhances the synergistic effects: a double act for the treatment of multidrug-resistant cancer. Biomater Sci. 2015; 3(1):163-174.

16. Zhao XY, Zhu YJ, Chen F, Wu J. Calcium phosphate nanocarriers dual-loaded with bovine serum albumin and ibuprofen: facile synthesis, sequential drug loading and sustained drug release. Chem Asian J. 2012; 7(7):1610-1615.

17. Nakamura A, Arimoto M, Takeuchi K, Fujii T. A rapid extraction procedure of human hair proteins and identification of phosphorylated species. Biol Pharm Bulletin. 2002; 25(5): 569-572.

18. Ramadan MF, Kroh LW, Morsel JT. Radical scavenging activity of black Cumin (*Nigella sativa* L), Coriander (*Coriandrum sativum* L), and Niger (*Guizotia abyssinica* Cass.) crude seed oils and oil fractions. J Agric Food Chem. 2003; 51: 6961–6969.

19. Tran TH, Ramasamy T, Cho HJ, Kim YI, Poudel BK, Choi HG, Yong CS, Kim JO. Formulation and optimization of raloxifene-loaded solid lipid nanoparticles to enhance oral bioavailability. J Nanosci Nanotechnol. 2014; 14(7): 4820–4831.

20. Atkinson AC, Donev AN. Optimum experimental designs. Oxford: Oxford University Press, 1992; 132–189.

21. Wu CC, Chen DH. Facile green synthesis of gold nanoparticles with gum arabic as a stabilizing agent and reducing agent. Gold Bulletin 2010; 43(4): 234–240.